Indolocarbazole Glycosides in Inactive Conformations

Michaël Facompré,[a] Carolina Carrasco,[a] Hervé Vezin,[b] John D. Chisholm,[c] Joshua C. Yoburn,[c] David L. Van Vranken,[c] and Christian Bailly*[a]

Indolocarbazole glycosides related to rebeccamycin represent a promising category of antitumor agents targeting DNA and topoisomerase I. These drugs prefer to adopt a closed conformation with an intramolecular hydrogen bond between the indole NH group and the pyranose oxygen atom. Three pairs of indolocarbazole monoglycosides bearing an NH or an N*-methyl indole moiety were synthesized and their biological properties investigated at the molecular and cellular level. Replacing the indole NH proton with a methyl group reduces DNA interaction and abolishes activity against DNA topoisomerase I. Surface plasmon resonance studies performed with a pair of water-soluble indolocarbazole glycosides and two hairpin oligonucleotides containing an* $[AT]_4$ *or a* $[CG]_4$ *sequence indicate that both the NH and the* N*-methyl derivative maintain a relatively high affinity for DNA (*$K_{eq} = 2-6 \times 10^5\ M^{-1}$*) but the incorporation of the methyl group restricts access to the DNA. The number of ligand binding sites (*n*) on the oligonucleotides is about twice as high for the NH compound compared to its* N*-methyl analogue. Modeling and* ^1H *NMR studies demonstrate that addition of the* N*-methyl group drives a radical change in conformation in which the orientation of the aglycone relative to the* β*-glucoside is reversed. The loss of the closed conformation by the* N*-methyl derivatives perturbs thir ability to access DNA binding sites and prevents the drug from inhibiting topoisomerase I. As a consequence, the NH compounds exhibit potent cytotoxicity against CEM leukemia cells with an* IC_{50} *value in the 1* μM *range, whereas the* N*-methyl analogues are 10 to 100 times less cytotoxic. These studies offer circumstantial evidence supporting the importance of the closed conformation in the interaction of indolocarbazole glycosides with their molecular targets, DNA and topoisomerase I.*

KEYWORDS:

anticancer agents · DNA binding · molecular modeling · NMR spectroscopy · topoisomerase I

Introduction

There are two broad classes of indolocarbazole glycoside natural products, represented by rebeccamycin and staurosporine.[1] In general, rebeccamycin and related compounds possessing a single glycosidic bond have been shown to inhibit the DNA cleavage and/or the kinase activities of topoisomerase I. Indolocarbazole glycosides related to rebeccamycin are currently involved in a number of phase II clinical trials targeting, for example, breast cancer, refractory neuroblastoma, non-Hodgkin's lymphoma, hepatobiliary carcinoma, and renal cell carcinoma. Staurosporine and related compounds, for which the indolocarbazole aromatic ring system is rigidly joined to the pyranose ring by two bonds (an *N*-glycosidic bond and an *N*,*O*-ketal), generally show no effect on topoisomerase I but are potent inhibitors of protein kinases such as protein kinases C (PKCs). In this series, the staurosporine derivatives UCN-01 and PKC-412, both currently in clinical development, show great promise as antitumor agents.[2–4]

With just a single *N*-glycosidic bond, rebeccamycin favors a single conformation in which the pyranose oxygen atom grips the indole NH group through an intramolecular hydrogen bond.[5] The preference for this hydrogen-bonded conformation is shared by rebeccamycin and the clinical candidate J-107088, even in solvents like dimethylsulfoxide (DMSO) that form strong hydrogen bonds.[6] Rebeccamycin has few degrees of freedom, so the forces that favor the closed conformation in solution are likely to favor the closed conformation when it is bound to its biological target.

Indole *N*-methyl derivatives of indolocarbazole ribosides, xylosides, arabinosides, galactosides, and lactosides have previously been prepared and shown to exhibit some growth

[a] *Dr. C. Bailly, M. Facompré, Dr. C. Carrasco*
INSERM U-524
et Laboratoire de Pharmacologie Antitumorale
du Centre Oscar Lambret, IRCL, Place de Verdun
59045 Lille (France)
Fax: (+33) 32016-9229
E-mail: bailly@lille.inserm.fr

[b] *Dr. H. Vezin*
Laboratoire de Chimie Organique Physique
URA CNRS 351, USTL Bât. C3
59655 Villeneuve d'Ascq (France)

[c] *Dr. J. D. Chisholm, J. C. Yoburn, Prof. D. L. Van Vranken*
Department of Chemistry
University of California, Irvine
California 92697 (USA)

  DOI: 10.1002/cbic.200200478

inhibitory activity against a human ovarian carcinoma cell line.[7] However, direct comparison shows that alkylation of the indole nitrogen atom of indolocarbazole glycosides leads to a substantial decrease in biological activity.[8] For example, the indolocarbazole glycoside **A** inhibits topoisomerase I and is

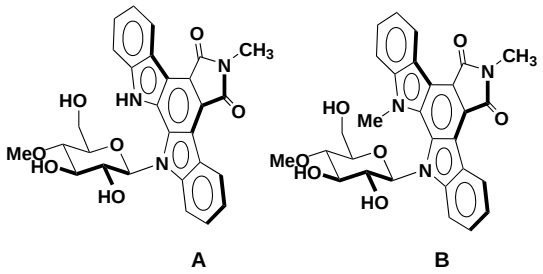

A **B**

active against a variety of bacterial and tumor cell lines (Table 1).[9] In contrast, when the indole NH proton is replaced with an *N*-methyl group, as in derivative **B**, the biological activity is severely compromised in all cases tested. Introduction of the indole *N*-methyl group reduces activity against topoisomerase I activity by at least a factor of 30 (Scheme 1).[9]

Replacing the indole NH proton of indolocarbazole glycosides with an *N*-methyl group is certain to prevent intramolecular hydrogen bonding. The β-glycosidic linkage of the sugar in rebeccamycin is essential for the DNA binding of rebeccamycin and its activity against topoisomerase I.[8] Thus, the pernicious effect of *N*-methylation on biological activity could result from a radical change in conformation. We set out to test this idea by investigating the effect of indole *N*-methylation on conformation using a combination of modeling and spectroscopic studies.

Table 1. *Biological activity of the indolocarbazole glycosides **A** and **B**.*

	A	B
topoisomerase 1[a]	0.6	> 19
Bacillus cereus[a]	1.6	> 19
P388 leukemia[b]	0.7	> 19
B16 melanoma[b]	1.1	8

[a] *Minimal inhibitory concentration (MIC)* [μM]. [b] IC_{50} [μM].

Results

Synthesis of the *N*-methyl derivative 3

The indole nitrogen atom of indolocarbazole glucoside **1** was *N*-methylated as shown in Scheme 1. As expected, the yield of the persilylation in the first step was poor,[10] but with some modifications the per-*O*-silylated derivative **2a** could be obtained in 33% yield. The remainder of the material was a mixture of two tris-silylated glycosides, which were inseparable. Alkylation of the indole nitrogen atom and deprotection of the silyl groups provided the modified indolocarbazole glycoside **3**.

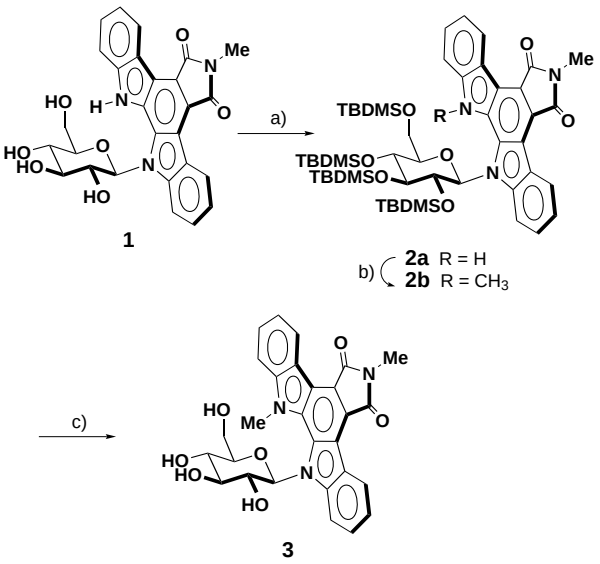

Scheme 1. *Synthesis of the methyl-indole derivative **3**. Experimental conditions: a) TBDMSOTf, Et_3N, DMAP, CH_2Cl_2, 22 h, 33%; b) NaH, MeI, THF, 94%; c) HCl, MeOH/$CHCl_3$, 72%. TBDMSOTf,* tert*-butyldimethylsilyltriflate; DMAP, 4-dimethylaminopyridine; THF, tetrahydrofuran.*

Solution conformations in dimethylsulfoxide

In ^{1}H NMR studies the *N*-methyl analogue **3** gave a single set of signals in DMSO-d_6. Double pulsed field gradient spin echo (DPFGSE) NOE experiments were used to assess the solution conformation of the two indolocarbazoles **1** and **3** (Scheme 2).

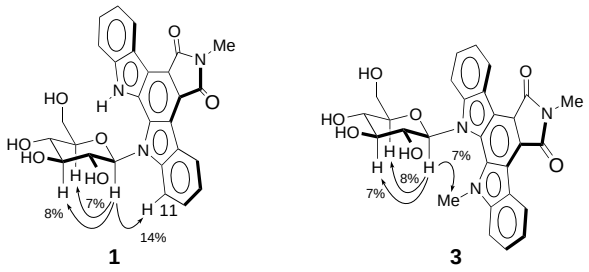

Scheme 2. *Solution data support the conformations shown. DPFGSE-NOEs (t_{mix} = 1.0 sec) define the conformation of indolocarbazole glycosides **1** and **3** in DMSO-d_6. Perceptage values refer to steady-state NOE enhancements.*

Irradiation of the methine proton at the anomeric position of **1** provided the expected 1,3-cross-ring enhancements plus a diagnostic NOE to H11 of the aromatic ring of the indolocarbazole. Irradiation of the corresponding methine proton at the anomeric position of **3** also led to the expected 1,3-cross-ring enhancements, but no enhancement of H11 was observed. Instead, an enhancement was observed at the indole *N*-methyl group. Thus, both of the indolocarbazole glucosides **1** and **3** adopt defined conformations but, while the parent glucosides adopt a closed conformation, the *N*-methyl derivative **3** adopts an open conformation. Presumably, modifications to the male-

imide ring, far from the sugar moiety, do not perturb this conformational preference.

Conformational and molecular orbital analyses

Molecular modeling was used to compare the conformation and electronic properties of compounds **1** (NH) and **3** (*N*-Me). Conformational analyses were performed on both structures by carrying out a Monte Carlo search with the MMF94 Force Field to find the global energy minima. The global minima were fully optimized by using Hartree-Fock theory with a 6 – 31G* basis set. As shown in Figure 1, the orientation of the carbohydrate residue differs significantly for the two molecules. The 5′-OH group on the sugar moiety of **1** is close to the indole NH proton, within hydrogen-bonding distance (1.96 Å). The same 5′-OH group in **3** projects from the opposite face of the molecule, far from the indolocarbazole chromophore. As a result, the dipole moments of the drugs were found to be very different: $\mu = 6.57$ and 3.34 Debye for **1** and **3**, respectively. These modeling results are in total agreement with the experimental NMR data showing that the orientation of the sugar residue is profoundly affected by substitution of the indole NH proton with a methyl group.

The molecular orbital analysis shows the spatial distribution of the highest occupied (E_{HOMO}, Figure 1 A) and lowest unoccupied molecular orbital (E_{LUMO}, Figure 1 B) throughout the molecules, as calculated by quantum mechanical methods at the ab initio 6 – 31G* level. The distribution of HOMO and LUMO energy is relatively similar for the two molecules, however, there is a slight difference for the band gap energy $\Delta\varepsilon = E_{HOMO} - E_{LUMO}$: -9.22 and -9.66 eV for **1** and **3**, respectively. The indole NH group of **1** appears as a zone of the molecule where electronic interaction is most likely to occur. This NH group may serve as an electron-withdrawing group. The electrostatic potential maps of the two molecules were also relatively similar (Figures 1 C and 2 d), but the closed, hydrogen-bonded structure exhibited significantly more negative charge in the aromatic π system than the open conformation of the *N*-methyl derivative. This polarization could enhance π-stacking interactions with electron-deficient rings. In both conformations, a high electrostatic density was observed for the sugar moiety and for the two carbonyl functions on the imide E-ring, which suggests that these groups probably participate in interactions with electron-poor regions of DNA bases and/or topoisomerase I.

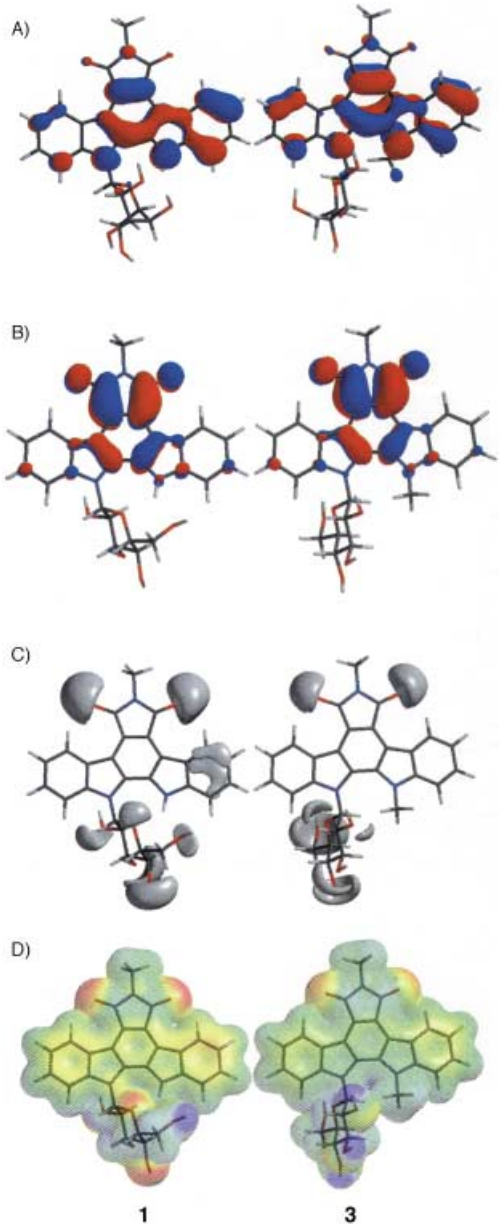

Figure 1. *Conformation and molecular orbital analysis for the most stable calculated configurations of **1** and **3**. a) HOMO and b) LUMO distribution; c) electrostatic potential map and d) electron density of the most stable calculated configurations of **1** and **3**.*

Synthesis of water-soluble analogues

Assuming the controlling effect of the indole *N*-methyl group, we set out to convert the *N*-methyl imides into analogues with better water solubility. We chose to append a diethylaminoethyl group to produce a structure analogous to the rebeccamycin derivative NSC655649. This compound, also known as BMS 181176, exhibits a broad antitumor activity in vitro against pediatric solid tumors[11] and has been evaluated in phase I clinical trials in both adult and pedriatric patients.[12, 13] The compound is currently undergoing phase II clinical trials for the treatment of ovarian and hepatobiliary cancers.[14] Initially, an attempt was made to form the diethylaminoethyl derivative of **1** through direct exchange by heating in neat *N*,*N*-diethylaminoethylamine, but after extensive heating only about half of the starting material had been converted. Alternatively, indolocarbazole glycoside **1** was first converted to the anhydride and then condensed with *N*,*N*-diethylaminoethylamine to form the desired imide in 54% overall yield (Scheme 3).[15] Overall, this three step anhydride method was not significantly better than the one-step exchange method. The free amine of **4** was converted to the hydrochloride salt with methanolic HCl. The

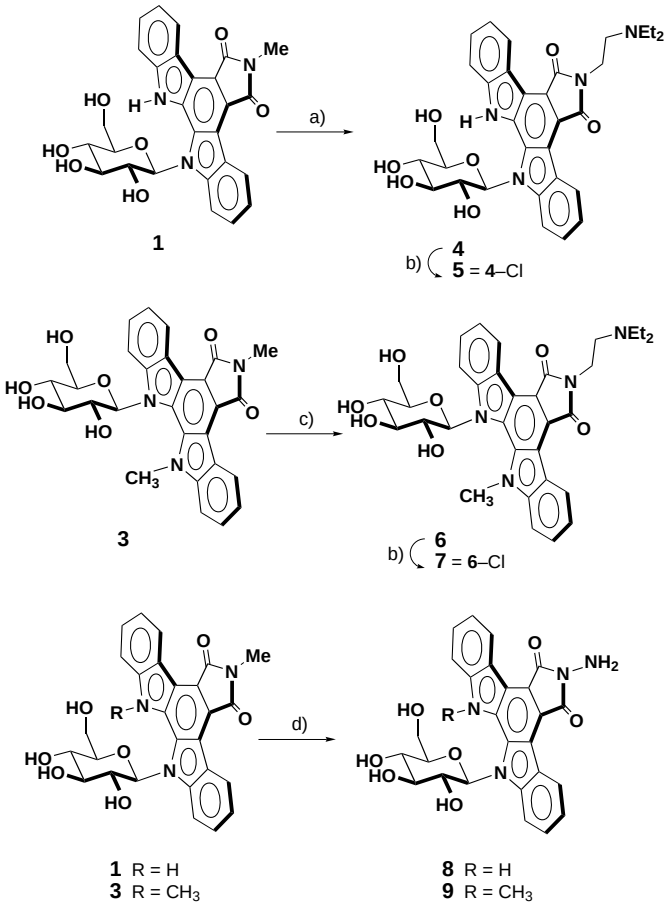

Scheme 3. N-*imide substitution. Experimental conditions: a) 1) KOH, aq. EtOH reflux, 2) conc. HCl, 3)* $Et_2NCH_2CH_2NH_2$*, DMF, 80 °C (yield 54% over 3 steps); b) HCl, MeOH/*$CHCl_3$*; c) neat* $Et_2NCH_2CH_2NH_2$*, 110 °C (yield 55%); d)* $NH_2NH_2 \cdot H_2O$*, 60 °C (yield* ***8****: 62%,* ***9****: 33%).*

N-diethylaminoethyl derivative **6** was formed directly through an imide exchange reaction with neat *N*,*N*-diethylaminoethylamine at 110 °C. As before, the free base was converted to the ammonium salt by using methanolic HCl. We next turned to formation of the *N*-amino imide derivatives by direct exchange. The corresponding *N*-methyl imides **1** and **3** were condensed with neat hydrazine hydrate to afford the desired *N*-amino imides **8** and **9**, respectively.[16]

DNA binding

Various spectrophotometric and biochemical techniques were employed to compare the DNA binding and topoisomerase I inhibition properties of the NH compounds **1**, **5** and **8** with those of the *N*-Me compounds **3**, **7** and **9**. First, DNA binding affinities were estimated by means of melting temperature experiments performed with poly(dAT)$_2$ in bis-phosphate ethylenediaminetetraacetate (BPE) buffer (16 mM Na^+ ions) at a drug/DNA-phosphate (D/P) ratio of 0.5. The ΔT_m values ($\Delta T_m = T_m^{complex} - T_m^{DNA}$) collated in Table 2 indicate that in all three cases, the NH compounds stabilize the polynucleotide duplex much more strongly than the corresponding *N*-Me compounds. Compounds

Table 2. *DNA binding and cytotoxicity.*

Compound	ΔT_m [°C][a] poly(dAT)$_2$	[AT]$_4$	IC_{50} [μM][b]
1	7.1	7.6	1.83
3	0	0	65.4
5	33.2	34.6	0.75
7	24.5	27	86.3
8	8	6.6	1.1
9	0	0	10.8

[a] Variation in melting temperature ($\Delta T_m = T_m^{complex} - T_m^{DNA}$). T_m measurements were performed in BPE buffer (6 mM Na_2HPO_4, 2 mM NaH_2PO_4, 1 mM EDTA; pH 7.1) with 10 μM drug and 20 μM DNA, either the alternating polymer poly(dAT)$_2$ or the hairpin oligomer containing the sequence [AT]$_4$, at 260 nm with a heating rate of 1 °C min^{-1}. [b] Drug concentration (μM) that inhibits the growth of leukemia CEM cells by 50% after incubation in liquid medium for 72 h.

1 and **8** markedly increased the melting temperature of the DNA, whereas **3** and **9** showed absolutely no effects. Compounds **5** and **7** both bear a cationic side chain that serves to anchor the drug on DNA; nevertheless, the stabilizing effect is considerably more pronounced with the NH derivative **5** than with the *N*-Me analogue **7**.

Additional T_m measurements were carried out with two hairpin oligonucleotides containing the duplex sequences [AT]$_4$ and [CG]$_4$. Biotinylated forms of these two oligomers were also used in the surface plasmon resonance (SPR) experiments described below. In BPE buffer the T_m of [AT]$_4$ and [CG]$_4$ are 34.7 °C and 84.8 °C, respectively. Therefore, only the AT sequence can be used to investigate drug binding. The ΔT_m values (Table 1) obtained with the AT oligomer are almost identical to those obtained with the long polymer poly(dAT)$_2$ and fully confirm that the methylation of the indole nitrogen considerably reduces the drug–DNA interaction process.

Compounds **1**–**3**, **8**, and **9** are sparingly soluble in water, in contrast to **5**–**7** for which concentrated stock solutions can be prepared in aqueous buffer without precipitation problems. As a result, these two cationic compounds were used in SPR studies to quantify more precisely their DNA binding strength. Two 5′-biotin-labeled hairpin oligomers containing an [AT]$_4$ or a [CG]$_4$ sequence were immobilized on the surface of a streptavidin-coated sensor chip and a blank flow cell was used as a control. To provide a signal directly proportional to the amount of bound compound, the reference response of this blank cell was substracted from the response in the DNA channel. Representative SPR sensorgrams at different concentrations of **5** and **7** binding to the AT and GC duplexes are shown in Figure 2. For both drugs the sensorgram results were fit in the steady-state region to calculate the binding constants. Direct binding plots (RU versus C_{free}) and the corresponding Scatchard plots (r/C_{free} versus r) are shown in Figure 3. The quantitative analyses gave the equilibrium binding constants (K_{eq}) listed in Table 3. The two compounds exhibit a roughly equal affinity for DNA, with binding constants of about $5-6 \times 10^5$ and $1-2 \times 10^5$ M^{-1} for the [AT]$_4$ and [CG]$_4$ sequences, respectively. The binding constants -

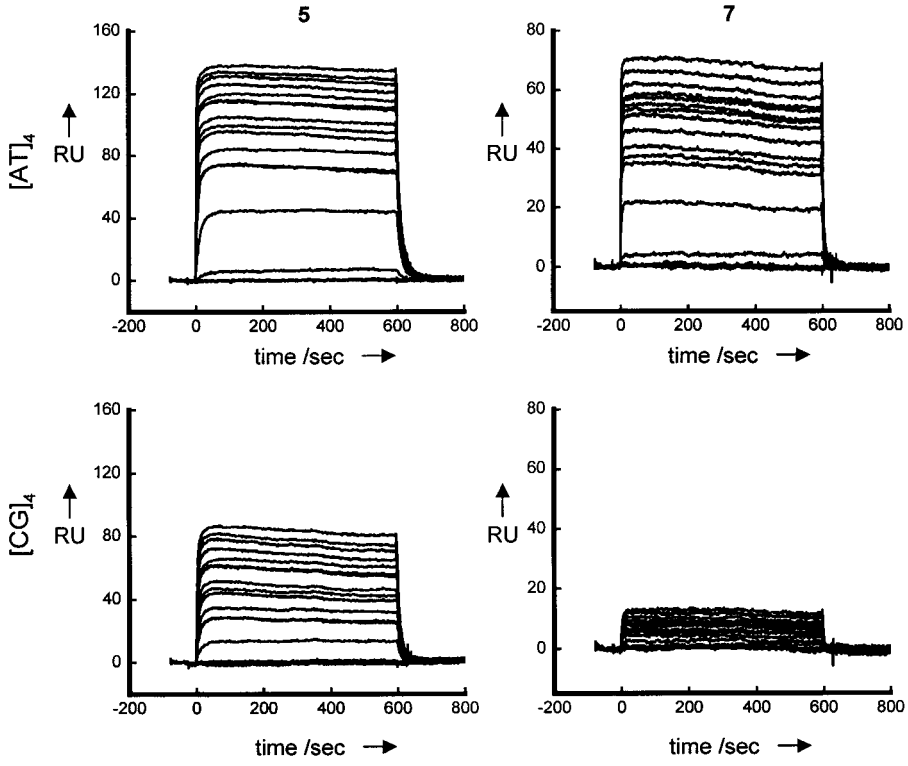

*Figure 2. SPR sensorgrams for binding of **5** and **7** to the $[AT]_4$ and $[CG]_4$ DNA hairpin oligomers in HBS-EP buffer. In each case, the concentration of the unbound ligand in the flow solution varies from 0 to 5 μM (top curve). RU = relative instrument response.*

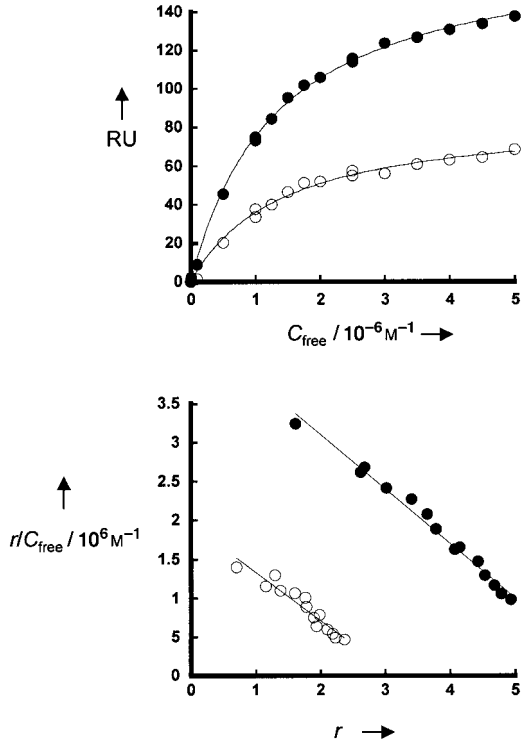

*Figure 3. Direct binding plots (RU versus C_{free}) and Scatchard plots (r/C_{free} versus r) used to determine the affinity constants for compounds **5** (●) and **7** (○) complexed with the $[AT]_4$ duplex. To construct these plots, RU values from the steady-state region of the SPR sensorgrams presented in Figure 2 were converted to r (moles drug bound/mole DNA hairpin) and plotted versus the concentration of unbound drug (C_{free}).*

are relatively high. For example, under strictly identical conditions, the uncharged glucosylindolocarbazole compound NB-506 was found to bind about eight times more weakly than **5** and **7** to the AT and GC duplexes.[17] The SPR data are in good agreement with the T_m data reported above. An important observation is that the binding stoichiometry (*n* values in Table 1) is significantly different for the two compounds. The CG and AT hairpin oligonucleotides, eight and nine base pairs in length respectively, offer one and three drug intercalation binding sites for the *N*-Me compound **7**. In contrast, the same oligonucleotides accommodate up to five molecules of the NH compound **5**. A parallel can be established between the number of molecules that bind and their shape, **5** being more compact whereas **7** presents a more extended and bulky configuration that limits its access to DNA intercalation sites.

***Table 3.** SPR binding parameters.*

Compound		K_{eq} [$\times 10^5$ M^{-1}][a]	n[b]
5	$[AT]_4$	6.62	5 – 6
	$[CG]_4$	1.36	5 – 6
7	$[AT]_4$	5.19	3
	$[CG]_4$	2.08	1

The DNA sequences show one strand of the duplex stem of the hairpin used in the BIAcore SPR experiments. Values determined for binding to the indicated DNA sequences in HBS buffer at 25 °C. [a] Equilibrium binding constant. [b] Number of compound binding sites on the DNA duplex.

Topoisomerase I inhibition

A conventional DNA relaxation assay with supercoiled plasmid DNA was used to evaluate the effects of the compounds on the catalytic activity of human topoisomerase I (Figure 4). The two compounds **5** and **7** bearing a diethylaminoethyl side chain do not stimulate DNA cleavage by topoisomerase I, essentially because their tight interaction with DNA (which reduces the electrophoretic mobility of supercoiled DNA) must restrict binding of the enzyme to its substrate. In contrast, the other compounds that bind more weakly to DNA showed a more or less pronounced effect on topoisomerase-I-mediated DNA

cleavage. The NH compounds **1** and **8** inhibit topoisomerase I but not the corresponding *N*-methyl analogues **3** and **9**.

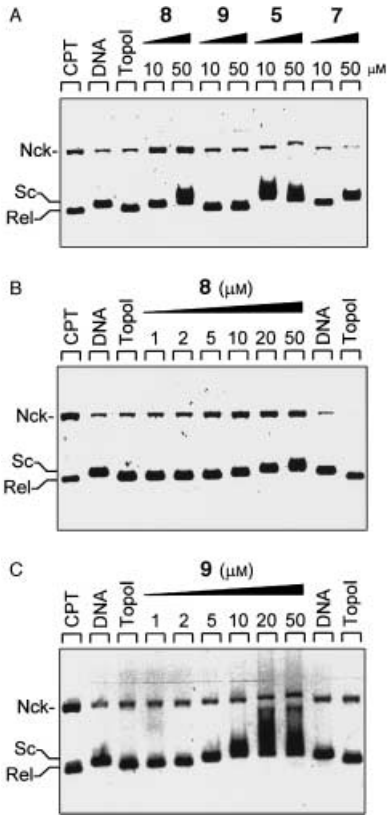

Figure 4. *Effect of the drugs on the relaxation of plasmid DNA by human topoisomerase I. In panel A, the drugs were tested at 10 and 50 μM. In panels B and C, compounds **8** and **9** were tested at increasing concentration from 1 to 50 μM, respectively. Native supercoiled pKMp27 DNA (0.5 μg; lane DNA) was incubated with 4 units topoisomerase I in the absence (lane Topol) or presence of drug at the indicated concentration (μM). Reactions were stopped by treatment with sodium dodecylsulfate and proteinase K. DNA samples were separated by electrophoresis on a 1% agarose gel. Camptothecin (CPT) was used at 50 μM. The gels were stained with ethidium bromide (1 μg mL^{-1}) and then photographed under UV light. Nck, nicked; Rel, relaxed; Sc, supercoiled.*

Compound **8** turned out to be a potent poison for the enzyme. This is shown in gel A in Figure 4 by a marked increase in the intensity of the band corresponding to nicked DNA molecules in the presence of **8** but not **9**. The effect of **8** is even more pronounced than that of the reference topoisomerase inhibitor camptothecin. A concentration-dependent analysis is shown in gels B and C (Figure 4). There is no doubt that **8** efficiently stabilizes topoisomerase I – DNA complexes in a concentration-dependent manner, whereas very little effect was seen with **9**.

To investigate the effect of the compounds on the sequence-specific cleavage of DNA by topoisomerase I, we employed two DNA restriction fragments of 117-bp and 72-bp, both uniquely labeled with ^{32}P at the 3′-end. In both cases, the radiolabeled DNA species were incubated with **8** and **9** in the presence of the enzyme and the resulting cleavage products were resolved on sequencing gels (Figure 5). A number of drug-induced topoisomerase I cleavage sites (arrows in Figure 5) were identified with **8** whereas, as with the plasmid DNA, no effect was observed with the methylated compound **9**. The cutting sites can be grouped into two categories: those which are common to the camptothecin derivative SN38 (the active metabolite of the

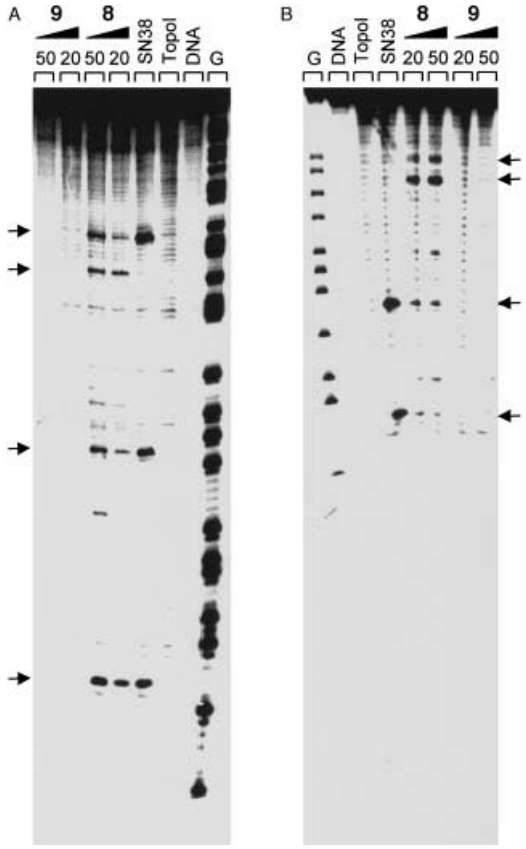

Figure 5. *Cleavage of the 117-mer (A) and the 72-mer DNA fragments (B) by human topoisomerase I in the presence of the indolocarbazoles **8** and **9**. In both cases, the 3′-end labeled fragment (DNA) was incubated in the absence (lane Topol) or presence of the test drug at the indicated μM concentration. Camptothecin (CPT) was used at 50 μM. Topoisomerase I cleavage reactions were analyzed on an 8% denaturing polyacrylamide gel. Numbers at the side of the gels show the nucleotide positions, determined with reference to the guanine tracks labeled G. The nucleotide positions and sequences of the cleavage sites are indicated.*

clinically used irinotecan) and correspond mainly to TG steps, and those specific to the indolocarbazole, which correspond to CG steps. The cleavage profiles seen with **8** are reminiscent of those previously obtained with related glycosyl indolocarbazoles.[18, 19] This second set of data fully confirms that the incorporation of a methyl group on the indole nitrogen abolishes the capacity of the drug to stabilize topoisomerase I – DNA complexes.

Cytotoxicity

A tetrazolium-based assay was applied to determine the drug concentration required to inhibit the growth of CEM human leukemia cells by 50% after incubation in the culture medium for 72 h (Table 1). The results are clear. The three NH compounds are

strongly cytotoxic with IC_{50} values in the low micromolar range whereas the *N*-Me derivatives are at least ten times less cytotoxic. In fact, **3** and **7** must be considered inactive with IC_{50} value above 50 μM. This result is therefore a solid indication that the indole *N*-methyl group is highly detrimental to cytotoxicity, a result consistent with previous biological studies with related analogues.[8, 9]

Discussion

We have synthesized indole *N*-methyl derivatives of indolocarbazole glycosides. Normally, bioactive indolocarbazole glycosides possess a closed conformation with a hydrogen bond between the indole NH proton and the pyranose oxygen atom. The N11-methyl group of the derivative excludes this interaction and destabilizes the closed rotamer by bumping into the pyranose oxygen atom. Spectroscopic studies in DMSO, a solvent that forms strong hydrogen bonds, show that the indole *N*-methyl group causes the aglycone to flip into a conformation that places the methyl group below rather than above the plane of the pyranose ring. The conformational changes induced by the N11 methyl group, and visualized in the modeling studies, are mirrored in the biological activity. Interestingly, the *N*-methylation does not reduce DNA binding affinity but affects the accessibility of the binding sites. The reduced number of binding sites on both the $[AT]_4$ and $[CG]_4$ oligomers observed with the *N*-methyl derivative **7** compared to its NH analogue **5** is without a doubt a direct consequence of the conformational change. The specific conformation of the *N*-methyl derivatives restricts access to DNA but also prevents inhibition of topoisomerase I. Unlike the NH compounds, the *N*-methyl analogues are no longer capable of stabilizing DNA – topoisomerase I covalent complexes and this probably explains their reduced cytotoxicity. Previous studies with different series of indolocarbazole glycosides have shown that topoisomerase I inhibition is generally an essential (but not unique) contributor to the antitumor activity of these drugs.[9, 20, 21] In terms of drug design, it seems clear that a closed conformation, that is an unsubstituted NH, must be considered if one wants to develop toposiomerase-I-targeted antitumor indolocarbazoles. Conversely, substitution of the NH group appears to be a simple and efficient strategy to eliminate topoisomerase I inhibition. The indole nitrogen atom thus acts as a molecular switch for the specific trapping of topoisomerase I.

An alternative strategy to modify the conformation of the glycoside residue with respect to the indolocarbazole chromophore involves conversion of the configuration of the *N*-glycosidic bond.[22] Previous studies have shown that an α anomer with an axial *N*-glycosidic linkage exhibits a drastically reduced affinity for DNA and fails to inhibit topoisomerase I. On the contrary, the corresponding β-anomer with an equatorial *N*-glycosidic linkage freely intercalates into DNA and potently stimulates DNA cleavage by topoisomerase I.[8] The configuration at the C1′ of the carbohydrate residue appears to control the insertion of the drug between base pairs. The structural effect of the introduced indole *N*-methyl group is more subtle because, by preventing the formation of the closed conformation, it restricts access to certain binding sites but does not diminish the strength of the interaction. The binding of rebeccamycin-type compounds to DNA can be modulated in different manners depending on the nature of the structural changes introduced at the drug level. In other words, one can tune the conformation of the indolocarbazole glycoside substrate to specifically modulate its interaction with the DNA receptor. The demonstration that the closed conformation is an essential structural element for the interaction of indolocarbazole glycosides with their molecular targets DNA and topoisomerase I is highly valuable for the rational design of antitumor drugs in this series.

In conclusion, the present study, which combines structural and biochemical approaches, provides a solid molecular basis to explain the different activity of NH and *N*-methyl indolo carbazole glycosides. Substitution of the indole NH proton with a methyl group leads to a radical change in conformation and prevents the formation of an H-bond-stabilized closed conformation which is essential for the ability of teh compound to access DNA binding sites and inhibit topoisomerase I.

Experimental Section

Chemistry: The synthesis of indolocarbazole glycoside **1** along with general procedures have been previously described.[5]

6-Methyl-12-[2,3,4,6-tetra-*O*-tert-butyldimethylsilyl-β-D-glucopyranosyl]indolo[2,3-*a*]pyrrolo[3,4-*c*]carbazole-5,7-dione (2a): Indolocarbazole glucoside **1** (140 mg, 0.279 mmol), triethyl amine (1 mL, 8.6 mmol), and DMAP (2 mg, 0.016 mmol) were suspended in CH_2Cl_2 (2 mL). TBDMSOTf (0.5 mL, 1.64 mmol) was then added. After 24 h, thin layer chromatography indicated incomplete reaction so more TBDMSOTf (0.5 mL, 1.64 mmol) was added. After 48 h the reaction mixture was poured into ethyl acetate, washed with 0.1 N HCl (3×), dried over Na_2SO_4, and concentrated. Purification by silica gel chromatography (hexane/ethyl acetate, 95:5) provided **2a** (87 mg, 33%) as a yellow solid. M.p.: 248–250 °C; $[\alpha]_D$: +72.5 (*c* = 0.9, THF); R_f = 0.44 (hexane/ethyl acetate, 90:10); IR (KBr): $\tilde{\nu}$ = 3374, 3058, 2934, 2892, 2859, 1755, 1704, 1579 cm^{-1}; ^1H NMR ($CDCl_3$, 500 MHz): δ = 10.16 (s, 1H), 9.30 (t, 2H, *J* = 8.6 Hz), 7.50–7.58 (m, 4H), 7.42 (t, 1H, *J* = 8.0 Hz), 7.38 (t, 1H, *J* = 8.0 Hz), 6.70 (d, 1H, *J* = 8.9 Hz), 4.41–4.46 (m, 3H), 4.25 (t, 1H, *J* = 9.5 Hz), 4.18 (br d, 1H, *J* = 3.0 Hz), 4.07 (dd, 1H, *J* = 9.2, 5.5 Hz), 3.33 (s, 3H), 1.10 (s, 9H), 1.02 (s, 9H), 0.92 (s, 9H), 0.89 (s, 3H), 0.50 (s, 9H), 0.30 (s, 3H), 0.27 (s, 3H), 0.25 (s, 3H), 0.15 (s, 3H), 0.11 (s, 3H), 0.10 (s, 3H), 0.89 (s, 3H), −0.43 (s, 3H), −1.34 (s, 3H) ppm; ^{13}C NMR ($CDCl_3$, 125 MHz): δ = 170.4, 170.2, 141.9, 140.3, 129.3, 127.4, 126.9, 126.8, 125.6, 125.5, 122.3, 122.1, 121.2, 120.8, 120.7, 119.3, 119.0, 118.1, 111.1, 110.2, 86.1, 82.2, 80.9, 77.8, 69.9, 63.2, 26.2, 25.9, 25.8, 25.3, 23.8, 18.4, 18.3, 17.9, 17.3, −3.7, −4.4, −4.5, −4.8, −5.2, −5.3, −6.5 ppm; MS (FAB$^+$): *m/z*: 957; HRMS (FAB$^+$): *m/z* calcd for $C_{52}H_{81}N_3O_7Si_4$: 958.5073 $[M+H]^+$; found: 958.5069; elemental analysis calcd (%) for $C_{52}H_{81}N_3O_7Si_4$: C 64.22, H 8.39, N 4.32; found: C 63.95, H 8.31, N 4.39.

6,13-Dimethyl-12-[2,3,4,6-tetra-*O*-*tert*-butyldimethylsilyl-β-D-glucopyranosyl]indolo[2,3-*a*]pyrrolo[3,4-*c*]carbazole-5,7-dione (2b): Protected indolocarbazole glucoside **2a** (87 mg, 0.09 mmol) and sodium hydride (60% dispersion, 92 mg, 2.3 mmol) were suspended in THF (2 mL). Iodomethane (100 μL, 1 mmol) was then added. After 1 h the reaction was cooled to 0 °C and quenched with sat. aq. NH_4Cl (1 mL). The reaction mixture was then taken up in ethyl acetate and

washed with brine (3×), dried over Na_2SO_4 and concentrated. Purification by silica gel chromatography (hexane/ethyl acetate, 95:5) provided **2b** (83 mg, 94%) as a yellow solid. M.p.: 270–272 °C; $[\alpha]_D$: −70.6 (c=0.8, THF); R_f=0.44 (hexane/ethyl acetate, 90:10); IR (KBr): $\tilde{\nu}$=2952, 2892, 1757, 1703, 1581 cm^{-1}; ^1H NMR ($CDCl_3$, 500 MHz): δ=9.27 (d, 1H, J=7.8 Hz), 9.24 (d, 1H, J=7.8 Hz), 7.95 (d, 1H, J=7.9 Hz), 7.62 (t, 1H, J=7.1 Hz), 7.48–7.50 (m, 2H), 7.41–7.45 (m, 2H), 6.50 (d, 1H, J=7.5 Hz), 4.49 (d, 1H, J=7.5 Hz), 4.39 (d, 1H, J=6.8 Hz), 4.22 (s, 3H), 4.20–4.22 (m, 1H), 4.07 (t, 1H, J=9.7 Hz), 4.01 (dd, 1H, J=9.5, 6.1 Hz), 3.90–3.91 (m, 1H), 3.32 (s, 3H), 1.53 (s, 9H), 1.08 (s, 9H), 0.98 (s, 18H), 0.22 (s, 3H), 0.19 (s, 3H), 0.13 (s, 3H), 0.12 (s, 3H), 0.10 (s, 3H), 0.07 (s, 3H), −0.50 (s, 3H), −1.37 (s, 3H) ppm; ^{13}C NMR ($CDCl_3$, 125 MHz): δ=170.1, 170.0, 146.0, 140.8, 133.5, 131.7, 127.6, 126.6, 125.9, 125.6, 124.6, 123.2, 122.2, 121.5, 120.9, 120.4, 120.0, 119.9, 114.9, 110.5, 87.2, 83.9, 78.0, 73.5, 69.0, 64.4, 35.5, 26.0, 25.9, 25.8, 24.8, 23.8, 18.4, 18.1, 18.0, 16.9, −3.6, −4.2, −4.4, −4.6, −4.9, −5.0, −5.1, −7.3 ppm; MS (FAB^+): m/z: 972; HRMS (FAB^+): m/z calcd for $C_{53}H_{83}N_3O_7Si_4$: 972.5229 $[M+H]^+$; found: 972.5242; elemental analysis calcd (%) for $C_{53}H_{83}N_3O_7Si_4$: C 64.52, H 8.48, N 4.26; found: C 64.23, H 8.42, N 4.37.

6,13-Dimethyl-12-[β-D-**glucopyranosyl]indolo[2,3-*a*]pyrrolo[3,4-*c*]-carbazole-5,7-dione** (**3**): Acetyl chloride (170 μL, 2.39 mmol) was added to MeOH (3 mL) to generate a solution of methanolic HCl. This solution was added to protected indolocarbazole glucoside **2b** (230 mg, 0.239 mmol) in $CHCl_3$ (1 mL). After 20 h the reaction was quenched with triethyl amine (0.5 mL), adsorbed on silica gel and purified by silica gel chromatography (ethyl acetate/MeOH, 90:10) to provide **3** (89 mg, 72%) as a yellow solid. M.p.: 340–344 °C; $[\alpha]_D$=+57.7 (c=0.35, DMSO); R_f=0.24 ($CHCl_3$/MeOH, 90:10); IR (KBr): $\tilde{\nu}$=3448, 2931, 2882, 1750, 1691, 1577 cm^{-1}; ^1H NMR ([D_6]DMSO, 500 MHz): δ=9.10 (d, 1H, J=8.3 Hz), 9.08 (d, 1H, J=8.2 Hz), 7.91 (d, 1H, J=8.2 Hz), 7.76 (d, 1H, J=8.2 Hz), 7.66 (t, 1H, J=7.8 Hz), 7.58 (t, 1H, J=7.6 Hz), 7.40–7.45 (m, 2H), 5.68 (d, 1H, J=8.7 Hz), 5.16 (d, 1H, J=5.2 Hz), 5.02 (d, 1H, J=5.3 Hz), 4.87 (t, 1H, J=5.9 Hz), 4.46 (d, 1H, J=5.8 Hz), 4.20 (s, 3H), 3.91 (dd, 1H, J=11.2, 5.5 Hz), 3.80 (q, 1H, J=8.6 Hz), 3.69–3.74 (m, 1H), 3.64–3.67 (m, 1H), 3.37–3.41 (m, 2H), 3.16 (s, 3H) ppm; ^{13}C NMR ([D_6]DMSO, 125 MHz): δ=170.2, 170.1, 145.4, 142.6, 133.1, 133.0, 128.5, 127.6, 125.7, 125.2, 125.1, 122.8, 122.6, 121.9, 120.9, 119.8, 119.6, 116.3, 112.0, 89.3, 80.7, 78.3, 70.7, 70.6, 62.0, 35.2, 24.6 ppm; MS (FAB^+): m/z: 516; HRMS (FAB^+): m/z calcd for $C_{28}H_{25}N_3O_7$: 515.1692; found: 515.1699

6-[*N*,*N*-Diethylaminoethyl]-12-[β-D-**glucopyranosyl]indolo[2,3-*a*]-pyrrolo[3,4-*c*]carbazole-5,7-dione** (**4**): A suspension of indolocarbazole glucoside **1** (100 mg, 0.199 mmol) in KOH (2 M, 3 mL) and ethanol (3 mL) was heated at reflux for 30 min and then cooled to room temperature. The reaction mixture was acidified with conc. HCl and extracted with ethyl acetate. The organic layer was washed with brine (3×), dried over Na_2SO_4, and concentrated in vacuo. The crude anhydride was taken up in 2 mL DMF and *N*,*N*-diethylaminoethylamine (100 mL, 710 mmol) was added. The mixture was heated at 80 °C for 20 h and then allowed to cool to room temperature. The reaction mixture was taken up in ethyl acetate, washed with sat. sodium bicarbonate (3×), dried over Na_2SO_4, and concentrated in vacuo. The imide was purified by silica gel chromatography (MeOH/conc. aq. NH_4OH/ethyl acetate, 10:1:89) to provide of imide **4** (64 mg, 54%) as a yellow solid. M.p.: 335 °C (decomp.); R_f=0.30 (MeOH/conc. aq. NH_4OH/ethyl acetate, 10:1:89); IR (KBr): $\tilde{\nu}$=3420, 3314, 2931, 1747, 1694, 1575 cm^{-1}; ^1H NMR ([D_6]DMSO, 500 MHz): δ=11.68 (s, 1H), 9.18 (d, 1H, J=8.0 Hz), 9.10 (d, 1H, J=8.0 Hz) 7.98 (d, 1H, J=8.5 Hz), 7.69 (d, 1H, J=8.1 Hz), 7.56–7.61 (m, 2H), 7.35–7.40 (m, 2H), 6.29 (d, 1H, J=9.0 Hz), 6.03 (brs, 1H), 5.41 (d, 1H, J=5.0 Hz), 5.16 (d, 1H, J=5.0 Hz), 4.93 (d, 1H, J=5.0 Hz), 4.08 (dd, 1H, J=10.7, 3.0 Hz), 3.94–4.03 (m, 2H) 3.81–3.83 (m, 3H), 3.50–3.63 (m, 2H), 2.76 (brs, 2H), 2.54 (brs, 2H), 2.09 (brs, 4H), 0.96 (brs, 6H) ppm; ^{13}C NMR ([D_6]DMSO, 125 MHz): δ=169.6, 169.5, 142.2, 140.9, 129.6, 128.3, 127.1, 127.0, 124.4 (2 signals), 121.4, 121.0, 120.7, 120.5, 120.0, 118.5, 118.3, 117.1, 112.2, 111.9, 84.5, 78.6, 76.6, 73.1, 67.6, 58.3, 49.9, 46.7, 35.6, 11.9 ppm; LRMS (ESI TOF): m/z: 587; HRMS (ESI TOF): m/z calcd for $C_{32}H_{35}N_4O_7^+$: 587.2506; found: 587.2485.

6-[*N*,*N*-Diethylaminoethyl]-12-[β-D-**glucopyranosyl]-13-methyl-indolo[2,3-*a*]pyrrolo[3,4-*c*]carbazole-5,7-dione** (**6**): A neat solution of **3** (58 mg, 0.113 mmol) in *N*,*N*-diethylaminoethylamine (3 mL) was heated at 110 °C for 19 h. The solvent was removed in vacuo and the residue was pre-adsorbed on silica gel prior to silica gel chromatography (MeOH/conc. aq. NH_4OH/ethyl acetate, 10:1:89) to give of **6** (38 mg, 58%) as a yellow solid. M.p.: 340 °C (decomp.); R_f=0.26 (MeOH/conc. aq. NH_4OH/ethyl acetate, 10:1:89); IR (KBr): $\tilde{\nu}$=3379, 3069, 2963, 1746, 1689, 1579 cm^{-1}; ^1H NMR ([D_6]DMSO, 500 MHz): δ=9.10 (t, 2H, J=8.0 Hz), 7.91 (d, 1H, J=8.0 Hz), 7.77 (d, 1H, J=7.7 Hz), 7.67 (t, 1H, J=8.0 Hz), 7.59 (t, 1H, J=8.0 Hz), 7.41–7.46 (m, 2H), 5.69 (d, 1H, J=8.8 Hz), 5.19 (brs, 1H) 5.03 (brs, 1H), 4.90 (brs, 1H) 4.48 (brs, 1H), 3.94 (d, 1H, J=11.2 Hz), 3.66–3.82 (m, 5H), 3.30–3.45 (m, 5H), 2.73, (t, 1H, J=6.4 Hz), 2.49–2.57 (m, 5H), 0.95 (t, 6H, J=1.9 Hz) ppm; ^{13}C NMR ([D_6]DMSO, 125 MHz): δ=169.5, 169.4, 144.9, 142.1, 132.6, 128.1, 127.1, 125.2, 124.7, 124.6, 122.3, 122.1, 121.6, 120.7, 119.3, 119.1, 119.0, 115.8, 111.6, 88.8, 80.2, 77.7, 70.2, 70.0, 61.4, 50.2, 47.0, 35.9, 12.2, 31.0 ppm; LRMS (ESI TOF): m/z: 601; HRMS (ESI TOF): m/z calcd for $C_{33}H_{37}N_4O_7^+$: 601.2662; found: 601.2663.

6-[*N*-amino]-12-[β-D-**glucopyranosyl]indolo[2,3-*a*]pyrrolo[3,4-*c*]-carbazole-5,7-dione** (**8**): *N*-methyl imide **1** (40 mg, 0.080 mmol) was dissolved in hydrazine hydrate (0.5 mL, 16.0 mmol) and the solution was warmed to 60 °C for 90 minutes. Upon cooling to room temperature, the reaction was diluted with water and extracted into ethyl acetate. The organic layers were pooled, washed with water, and then dried over Na_2SO_4. Concentration in vacuo provided an orange oil, which was adsorbed on silica gel (1 g) with ethyl acetate and MeOH. Silica gel chromatography (MeOH/acetate, 0:100 to 15:85) provided 25 mg (62.4%) of *N*-amino imide **8** as an orange solid. *N*-amino imide **8**: M.p.: 296–299 °C; R_f=0.33 (ethyl acetate/MeOH, 90:10); IR (KBr): $\tilde{\nu}$=3321, 2928, 2239, 1738, 1681, 1571, 1452, 1386, 1329, 1229, 1076, 1005, 743, 638 cm^{-1}; ^1H NMR ([D_6]DMSO, 500 MHz, 294 K): δ=11.66 (s, 1H), 9.19 (d, 1H, J=10.0 Hz), 9.11 (d, 1H, J=5.0 Hz), 7.98 (d, 1H, J=10.0 Hz), 7.69 (d, 1H, J=5.0 Hz), 7.58 (m, 3H), 7.38 (dd, 2H, J=14.4, 7.3 Hz), 6.28 (d, 1H, J=5.0 Hz), 6.04 (t, 1H, J=5.0 Hz), 5.44 (d, 1H, J=5.0 Hz), 5.17 (d, 1H, J=5.3 Hz), 5.00 (brs, 2H), 4.94 (d, 1H, J=5.2 Hz), 4.07 (dd, 1H, J=11.0, 3.8 Hz), 3.95–4.01 (m, 2H), 3.82 (dd, 1H, J=7.3, 2.9 Hz), 3.52–3.60 (m, 2H) ppm; ^{13}C NMR ([D_6]DMSO, 125 MHz, 298 K): δ=169.5, 169.3, 142.9, 141.6, 130.3, 128.9, 127.8, 127.6, 125.0, 122.1, 121.7, 121.3, 121.1, 119.1, 118.9, 117.7, 117.2, 112.9, 112.5, 85.1, 79.3, 77.3, 73.8, 68.2, 68.0, 59.0 ppm; LRMS (ESI TOF): m/z: 525.

6-[*N*-amino]-12-[β-D-**glucopyranosyl]-13-methyl-indolo[2,3-*a*]pyrrolo[3,4-*c*]carbazole-5,7-dione** (**9**): *N*-methyl imide **3** (15 mg, 0.030 mmol) was dissolved in hydrazine hydrate (0.5 mL, 16.0 mmol) and the solution was warmed to 60 °C for 60 minutes. Upon cooling to room temperature, the reaction was diluted with water and extracted into ethyl acetate. The organic layers were pooled, washed with water, and then dried over Na_2SO_4. Concentration in vacuo provided a yellow oil which was adsorbed on silica gel (1 g) by using ethyl acetate and MeOH. Silica gel chromatography (10 g, ethyl acetate/MeOH, 100:0 to 20:80) provided *N*-amino imide **9** (5 mg, 33.3%) as a yellow solid. *N*-amino imide **9**: M.p.: 333–335 °C; R_f=0.26 (ethyl acetate/MeOH, 90:10); IR (KBr): $\tilde{\nu}$=3416, 2919, 1752, 1700, 1643, 1571, 1462, 1386, 1324, 1205, 1029, 748, 443 cm^{-1}; ^1H NMR ([D_6]DMSO, 500 MHz, 298 K): δ=9.15 (dd, 2H, J=7.5, 7.5 Hz, 7.95 (d, 1H, J=8.2 Hz), 7.80 (d, 1H, J=8.3 Hz), 7.72 (dd, 1H, J=7.2,

7.2 Hz), 7.64 (dd, 1 H, *J* = 8.2, 8.2 Hz), 7.49 (ddd, 2 H, *J* = 7.0, 7.2, 3.6 Hz), 5.72 (d, 1 H, *J* = 8.7 Hz), 5.21 (d, 1 H, *J* = 5.2 Hz), 5.05 (d, 1 H, *J* = 5.4 Hz), 5.01 (br s, 2 H), 4.90 (t, 1 H, *J* = 5.8 Hz), 4.51 (d, 1 H, *J* = 5.8 Hz), 4.23 (s, 3 H), 3.95 (dd, 1 H, *J* = 11.3, 6.3 Hz), 3.83 (m, 1 H), 3.66–3.78 (m, 3 H); LRMS (ESI TOF): *m/z:* 539; ESI MS: *m/z* calcd for $C_{27}H_{24}N_4O_7Na$ [*M* + Na]$^+$: 539.1543, found: 539.1527.

Computational chemistry: All calculations were performed on a NT workstation (PIII-650 MHz processor) with the Spartan Pro V 1.0.1 software package. A conformational analysis was performed for **1** and **3** on all rotatable bonds by using the Monte Carlo procedure implemented in the Spartan package. The resulting structures were minimized with a MMF94 force field and fully optimized at the ab initio RHF/6–31G* level.

Drugs, chemicals, and biochemicals: Camptothecin was purchased from Sigma. It was first dissolved in DMSO at 5 mM and then further diluted with water. In the cleavage reactions the final DMSO concentration never exceeded 0.3% (v/v). Under these conditions DMSO which is also used in the controls, does not affect the topoisomerase activity. The stock solutions of drugs were kept at −20 °C and freshly diluted to the desired concentration immediately prior to use. All other chemicals were analytical grade reagents. Restriction endonucleases and AMV reverse transcriptase were purchased from Roche and used according to the supplier's recommended protocol in the activity buffer provided. The double-stranded polynucleotide poly(dAT)$_2$ was purchased from Pharmacia. All solutions were prepared with double deionised, Millipore filtered water.

Melting temperature studies: Melting curves were measured on an Uvikon 943 spectrophotometer coupled to a Neslab RTE111 cryostat. For each series of T_m measurements, 12 samples were placed in a thermostatically controlled cell holder, and the quartz cuvettes (10-mm pathlength) were heated by circulating water. The measurements were performed in BPE buffer (6 mM Na_2HPO_4, 2 mM NaH_2PO_4, 1 mM EDTA; pH 7.1). The temperature inside the cuvette was measured with a platinum probe; the temperature was increased over the range 20–100 °C with a heating rate of 1 °C min^{-1}. The "melting" temperature T_m was taken as the mid-point of the hyperchromic transition.

Surface plasmon resonance (SPR): Two 5′-biotin labeled DNA hairpins (Eurogentec, PAGE purified) were used in surface plasmon resonance studies (hairpin loop underlined): d(biotin-CATATA-TATCCCCATATATATG) and d(biotin-CGCGCGCGTTTTCGCGCGCG). Samples of hairpin DNA oligomers in HBS-EP buffer at 25 nM concentration were applied to flow cells in streptavidin derivatized sensor chips (BIAcore SA-chips) by direct flow at 2 μL min^{-1} in a four-channel Biacore 3000 optical biosensor system. The sensor chips were conditioned with three consecutive 1-min injections of 1 M NaCl in 50 mM NaOH, followed by extensive washing with buffer. Nearly the same amount of all oligomers were immobilized on the surface by non covalent capture, with one of the flow cells left blank as a control. Manual injection was used with a flow rate of 2 μL min^{-1} to achieve long contact times with the surface and to control the amount of the DNA bound to the surface. All procedures for binding studies were automated as methods that use repetitive cycles of sample injection and regeneration. Steady-state binding analysis was performed with multiple injections of different compound concentrations over the immobilized DNA surfaces for a 10-min period at a flow rate of 20 μL min^{-1} and at 4 or 25 °C. Drug solutions with known concentrations were prepared in filtered and degassed buffer by serial dilutions from stock solutions and were injected from 7-mm plastic vials with pierceable plastic crimp caps (Biacore Inc.).

The instrument response (RU) in the steady-state region is proportional to the amount of bound drug and was determined by linear averaging over an 80-s time span. The predicted maximum response per bound compound in the steady-state region (RU_{max}) is determined from the DNA molecular weight, the amount of DNA on the flow cell, the compound molecular weight, and the refractive index gradient ratio of the compound and DNA.[23] In the present case, the observed RU values at high concentrations are greater than RU_{max}, which points to the existence of several binding sites in these DNA sequences. The number of binding sites (n) was determined from Scatchard plots derived from plots of RU/concentration versus RU, plot by using a linear regression analysis (data not shown). The RU_{max} value is required to convert the observed response (RU) to the standard binding parameter, r (moles drug bound/moles DNA hairpin) by using the equation:

$$r = \frac{RU}{RU_{max}}$$

Average fitting of the sensorgrams at the steady-state level was performed with the BIAevaluation 3.0 program. To obtain the affinity constants, the results from the steady-state region were fitted with a multiple-equivalent-site model by using the Kaleidagraph program for nonlinear least squares optimization of the binding parameters with the following equation:

$$r = \frac{n \times K \times C_{free}}{(1 + K \times C_{free})}$$

where K, the macroscopic binding constant, is one variable to fit, r represents the moles of bound compound per mole of DNA hairpin duplex,[24] C_{free} is the concentration of the compound in equilibrium with the complex and is fixed by the concentration in the flow solution, n is the number of compound binding sites on the DNA duplex and is the second variable to fit. The r values are calculated from the ratio RU/RU_{max}, where RU is the steady-state response at each concentration and RU_{max} is the predicted RU for binding of a single compound to the DNA on a flow cell.

DNA relaxation experiments: Supercoiled pKMp27 DNA (0.5 μg) was incubated with human topoisomerase I (4 units, TopoGen Inc.) at 37 °C for 1 h in relaxation buffer (50 mM Tris pH 7.8, 50 mM KCl, 10 mM $MgCl_2$, 1 mM dithiothreitol, 1 mM EDTA) in the presence of varying concentrations of the drug under study. Reactions were terminated by adding SDS to 0.25% and proteinase K to 250 μg mL^{-1}. DNA samples were then added to the electrophoresis dye mixture (3 μL) and electrophoresed in a 1% agarose gel at room temperature for 2 h at 120 V. Gels contained ethidium bromide (1 μg mL^{-1}) and were washed with water prior to being photographed under UV light.[25]

Purification and radiolabeling of DNA restriction fragments: The 117- and 72-bp DNA fragments were prepared by 3′-[^{32}P]-end labeling of the *Eco*RI-*Pvu*II double digest of the plasmid pBS by using γ-[^{32}P]-dATP (3000 Ci mMol^{-1}) and AMV reverse transcriptase. The same procedure was applied for the 174-mer *Eco*RI-*Pvu*II fragment from plasmid pKS. In each case, the digestion products were separated on a 6% polyacrylamide gel under native conditions in TBE buffered solution (89 mM Tris-borate pH 8.3, 1 mM EDTA). After autoradiography, the band of DNA was excised, crushed, and soaked in water overnight at 37 °C. This suspension was filtered through a Millipore 0.22-μm filter and the DNA was precipitated with ethanol. Following washing with 70% ethanol and vacuum drying of the

precipitate, the labeled DNA was resuspended in 10-mM Tris buffer adjusted to pH 7.0 and containing 10 mM NaCl.

Sequencing of topoisomerase-I-mediated DNA cleavage sites: Each reaction mixture contained 3′-[^{32}P]-end-labeled DNA (2 μL, ~1 μM), water (5 μL), 10X topoisomerase I buffer (2 μL), and drug solution at the desired concentration (10 μL, 1 – 50 μM). After 10-min incubation to ensure equilibration, the reaction was initiated by addition of topoisomerase I (2 μL, 4 units; Life Technologies). Samples were incubated for 45 min at 37 °C prior to addition of SDS to 0.25% and proteinase K to 250 μg mL^{-1} to dissociate the drug-DNA-topoisomerase I cleavable complexes. The DNA was precipitated with ethanol and then resuspended in formamide-TBE loading buffer (5 μL), denatured at 90 °C for 4 min, then chilled in ice for 4 min prior to loading on to the sequencing gel. DNA cleavage products were resolved by polyacrylamide gel electrophoresis under denaturating conditions (0.3 mm thick, 8% acrylamide containing 8 M urea). After electrophoresis (about 2.5 h at 60 W, 1600 V in Tris-Borate-EDTA buffered solution), gels were soaked in 10% acetic acid for 10 min, transferred to Whatman 3MM paper, and dried under vacuum at 80 °C. A Molecular Dynamics 425E PhosphorImager was used to collect data from the storage screens exposed to dried gels overnight at room temperature. Base line-corrected scans were analyzed by integrating all the densities between two selected boundaries with ImageQuant version 3.3 software. Each resolved band was assigned to a particular bond within the DNA fragments by comparison of its position relative to sequencing standards generated by treatment of the DNA with dimethylsulphate followed by piperidine-induced cleavage at the modified guanine bases in this DNA (G-track).

Cell cultures and survival assay: Human CEM leukemia cells were obtained from the American Tissue Culture Collection (ATCC number: CCL-119). Cells were grown at 37 °C in a humidified atmosphere containing 5% CO_2 in RPMI 1640 medium, supplemented with 10% fetal bovine serum, L-glutamine (2 mM), sodium bicarbonate (1.5 g L^{-1}), glucose (4.5 g L^{-1}), HEPES (10 mM), sodium pyruvate (1 mM), penicillin (100 IU mL^{-1}), and streptomycin (100 μg mL^{-1}). The cytotoxicity of the test compounds was assessed by using a cell proliferation assay developed by Promega (CellTiter 96 AQ_{ueous} one solution cell proliferation assay). Briefly, 3×10^4 exponentially growing cells were seeded in 96-well microculture plates with various drug concentrations in a volume of 100 μL. After 72 h incubation at 37 °C, tetrazolium dye (20 μL) was added to each well and the samples were incubated for a further 2 h at 37 °C. Plates were analyzed on a Labsystems Multiskan MS (type 352) reader at 492 nm.

This work was supported by grants to C.B. from the Ligue Nationale Contre le Cancer (Equipe labellisée LA LIGUE) and to D.L.V.V. from the American Cancer Society, and by a Marie Curie Fellowship of the European Community Program "Improving Human Research Potential and the Socio-economic Knowledge Base" under contract number "HPMFCT-2000 – 00701 to C.C. We thank the Institut de Médecine Préventive et Recherche Thérapeutique for access to the BIAcore 3000 instrumentation and Prof. W. D. Wilson (Department of Chemistry, Georgia State University, Atlanta) for expert assistance with the SPR experiments.

[1] C. Bailly in *Small Molecule DNA and RNA Binders* (Eds.: M. Demeunynck, C. Bailly, W. D. Wilson), Wiley-VCH, Weinheim, **2003**, Vol. 2, 538 – 575.
[2] P. Thavasu, D. Propper, A. McDonald, N. Dobbs, T. Ganesan, D. Talbot, J. Braybrook, F. Caponigro, C. Hutchison, C. Twelves, A. Man, D. Fabbro, *Cancer Res.* **1999**, *59*, 3980 – 3984.
[3] D. Fabbro, S. Ruetz, S. Bodis, M. Pruschy, K. Csermak, A. Man, P. Campochiaro, J. Wood, T. O'Reilly, T. Meyer, *Anti-Cancer Drug Des.* **2000**, *15*, 17 – 28.
[4] S. Akinaga, K. Sugiyama, T. Akiyama, *Anti-cancer Drug Des.* **2000**, *15*, 43 – 52.
[5] E. J. Gilbert, J. D. Chisholm, D. L. Van Vranken, *J. Org. Chem.* **1999**, *64*, 5670 – 5676.
[6] A. Akao, S. Hiraga, T. Iiada, A. Kamatani, M. Kawasaki, T. Mase, T. Nemoto, N. Satake, S. A. Weissman, D. M. Tschaen, K. Rossen, D. Petrillo, R. A. Reamer, R. P. Volante, *Tetrahedron* **2001**, *57*, 8917 – 8923.
[7] A. A. Bakhmedova, L. D. Garaeva, O. V. Goryunova, T. D. Miniker, I. L. Plikhtyak, L. V. Ektova, V. M. Adanin, T. P. Ivanova, I. V. Yartseva, S. Y. Melnik, *Russ. J. Bioorg. Chem.* **1997**, *23*, 608 – 615.
[8] C. Bailly, X. G. Qu, D. E. Graves, M. Prudhomme, J. B. Chaires, *Chem. Biol.* **1999**, *6*, 277 – 286.
[9] P. Moreau, F. Anizon, M. Sancelme, M. Prudhomme, C. Bailly, C. Carrasco, M. Ollier, D. Sevère, J. F. Riou, D. Fabbro, T. Meyer, A. M. Aubertin, *J. Med. Chem.* **1998**, *41*, 1631 – 1640.
[10] T. Halmos, R. Montserret, J. Filippi, K. Antonakis, *Carbohydr. Res.* **1987**, *170*, 57 – 69.
[11] S. Weitman, R. Moore, H. Barrera, N. K. Cheung, E. Izbicka, D. D. Van Hoff, *J. Pediatr. Hematol. Oncol.* **1998**, *20*, 136 – 139.
[12] A. W. Tolcher, S. G. Eckhardt, J. Kuhn, L. Hammond, G. Weiss, J. Rizzo, C. Aylesworth, M. Hidalgo, A. Patnaik, G. Schwartz, S. Felton, E. Campbell, E. K. Rowinsky, *J. Clin. Oncol.* **2001**, *19*, 2937 – 2947.
[13] A. Dowlati, C. L. Hoppel, S. T. Ingalls, S. Majka, X. L. Li, N. Sedransk, T. Spiro, S. L. Gerson, P. Ivy, S. C. Remick, *J. Clin. Oncol.* **2001**, *19*, 2309 – 2318.
[14] J. Merchant, K. Tutsch, A. Dresen, R. Arzoomanian, D. Alberti, C. Feierabend, K. Binger, R. Marnoccha, J. Thomas, J. Cleary, G. Wilding, *Clin. Cancer Res.* **2002**, *8*, 2193 – 2201.
[15] T. B. Lowinger, C. Jingxi, P. L. Spence, *Tetrahedron Lett.* **1995**, *36*, 8383 – 8386.
[16] E. R. Pereira, L. Belin, M. Sancelme, M. Prudhomme, M. Ollier, M. Rapp, D. Severe, J. F. Riou, D. Fabbro, T. Meyer, *J. Med. Chem.* **1996**, *39*, 4471 – 4477.
[17] C. Carrasco, H. Vezin, W. D. Wilson, J. Ren, J. B. Chaires, *Anti-Cancer Drug Des.* **2001**, *16*, 99 – 107.
[18] C. Bailly, J. F. Riou, P. Colson, C. Houssier, E. Rodrigues-Pereira, M. Prudhomme, *Biochemistry* **1997**, *36*, 3917 – 3929.
[19] C. Bailly, L. Dassonneville, P. Colson, C. Houssier, K. Fukasawa, S. Nishimura, T. Yoshinari, *Cancer Res.* **1999**, *59*, 2853 – 2860.
[20] F. Kanzawa, K. Nishio, N. Kubota, N. Saijo, *Cancer Res.* **1995**, *55*, 2806 – 2813.
[21] Y. Urasaki, G. Laco, Y. Takebayashi, C. Bailly, G. Kohlhagen, Y. Pommier, *Cancer Res.* **2001**, *61*, 504 – 508.
[22] F. Anizon, L. Belin, P. Moreau, M. Sancelme, A. Voldoire, M. Prudhomme, M. Ollier, D. Sevère, J. F. Riou, C. Bailly, D. Fabbro, T. Meyer, *J. Med. Chem.* **1997**, *40*, 3456 – 3465.
[23] T. M. Davis, W. D. Wilson, *Anal. Biochem.* **2000**, *284*, 348 – 353.
[24] K. A. Connors, *Binding Constants: The Measurement of Molecular Complex Stability*, Wiley, New York, **1987**.
[25] C. Bailly, *Methods Enzymol.* **2001**, *340*, 610 – 623.

Received: August 21, 2002
Revised version: February 14, 2003 [F478]

